

# Polarisation characteristics of optical rib waveguides

ADAM MAJEWSKI

Institute of Electronic Systems, Warsaw University of Technology, ul. Nowowiejska 15/19, 00-665 Warszawa, Poland.

SŁAWOMIR SUJECKI

Department of Electrical and Electronic Engineering, University of Nottingham, University Park, Nottingham NG7 2RD, UK.

The polarisation characteristics of optical rib waveguides fabricated on the basis of semiconductor and polymer materials are analysed. In particular, the influence of the dimensions and refractive indices on the value of birefringence and the field distributions are investigated. Moreover, the ways of minimizing the value of modal birefringence in large optical waveguides are studied.

## 1. Introduction

Optical rib waveguides have found many applications in integrated optics circuits. Currently the most attractive structures seem to be the rib waveguides made of semiconductor materials, namely silicon (Si) and gallium arsenide (GaAs), as they can be utilised for fabrication of Optoelectronic Integrated Circuits (OEIC), *i.e.*, electronic and optic circuits integrated together on one substrate.

The cross-section of an optical rib waveguide is shown in Fig. 1. The structure consists of two dielectric layers of refractive index  $n_f$  and  $n_c$ , which are deposited on the substrate of the refractive index  $n_s$ . The area inside the core of the rib waveguide, above the dashed horizontal line,  $y > h$ , is called the rib. The slab waveguide of the height  $H$  (domain 1 in Fig. 1) is frequently referred to in the literature as inner slab, whereas the slab waveguide of height  $h$  (outside domain 1 in Fig. 1), is named outer slab. If for a rib waveguide the height  $h$  is much larger than the wavelength, it is called a large rib waveguide [1]. The single-mode condition for large rib waveguides is given by the following inequality [1]:

$$\frac{2W}{H} \leq 0.3 + \frac{h/H}{\sqrt{1 - (h/H)^2}}. \quad (1)$$

An example of a large rib waveguide is silicon on insulator (SOI) structure [2]. The cross-section of a SOI rib waveguide is shown in Fig. 2a. The isolation layer of  $\text{SiO}_2$  has been made on the silicon substrate. The thickness of this layer should be large enough to prevent the guided modes from leakage into substrate. When  $h > 1 \mu\text{m}$ , the layer of  $0.2 \mu\text{m}$  is sufficient [2]. Although the refractive index difference

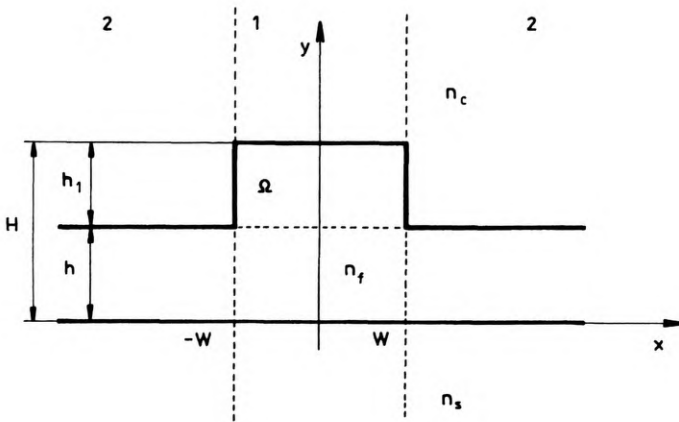


Fig. 1. Cross-section of a rib optical waveguide

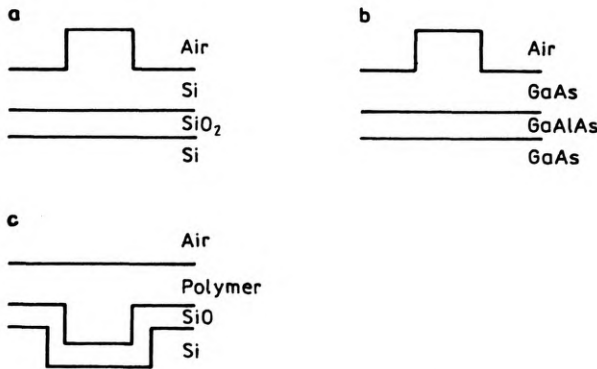


Fig. 2. Rib optical waveguides: a – SOI, b – on GaAs substrate, c – polymer on Si substrate

between core and cladding is large the SOI rib waveguide can be efficiently coupled with a single-mode fiber, which is one of its advantages [3].

The dimensions of GaAs based rib waveguides are comparable with the wavelength [4]. An example of a GaAs rib structure is shown in Fig. 2b. In this case, the isolation from the substrate is provided by an GaAlAs layer. The refractive index difference between core and substrate depends on the form of the GaAlAs alloy. For example, the refractive indices of  $\text{Ga}_{0.92}\text{Al}_{0.08}\text{As}$  and GaAs, at the wavelength of  $1.15 \mu\text{m}$ , are *ca.* 3.4 and 3.44, respectively.

Recently, intensive research on polymer rib waveguides has been conducted because these structures are potentially cheaper in mass production. A successful polymer rib waveguide fabrication on a silicon substrate (Fig. 2c), with propagation losses below  $0.5 \text{ dB/cm}$ , has already been demonstrated [5]. The polymer material used was benzocyclobutene (BCB), which exhibits good mechanical properties and thermal stability [5].

## 2. Results and discussion

For the purpose of analysis, a mode solver based on the semivectorial finite difference method [6] has been employed, as the method is very general and can produce accurate results for a wide variety of rib waveguide structures [6], [7], in particular the ones which are discussed in this paper.

It has been assumed that the refractive index of silicon and silicon dioxide at the wavelength of 1.3  $\mu\text{m}$  is 3.5 and 1.45, respectively, and 1.54 in the case of the BCB polymer.

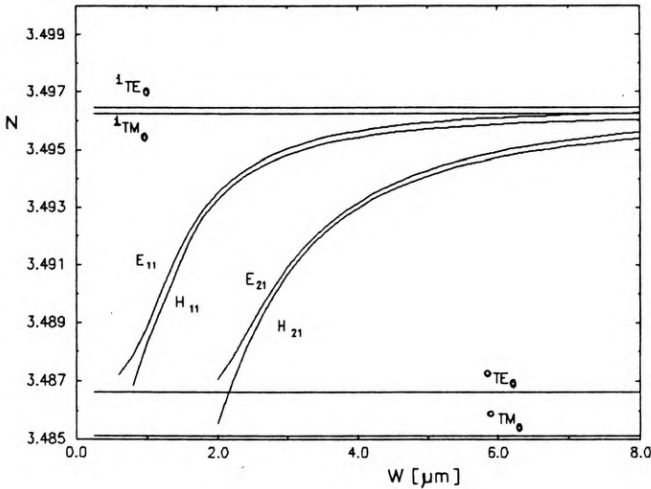


Fig. 3. Dependence of the effective index of a SOI rib waveguide on the width  $W$  where  $h = 2 \mu\text{m}$ ,  $H = 4 \mu\text{m}$  at the wavelength of 1.3  $\mu\text{m}$

In Figure 3, the dependence of the effective index  $N = \beta/k$  on width  $W$ , where  $\beta$  is the propagation constant and  $k$  – the wavelength, for a typical SOI rib waveguide structure is presented. The  ${}^i\text{TE}_m$  and  ${}^i\text{TM}_m$  denote effective index values of  $m$ -th order mode of the inner slab (superscript  $i$ ) or the outer slab (superscript  $o$ ), (Fig. 3). It is seen that as the width  $W$  increases, the values of  $N$  for  $E_{11}$  and  $H_{11}$  modes tend to the values of the effective index of the fundamental TE and TM mode of the inner slab, respectively. If the width decreases, they tend to the respective values of the effective indices of the outer slab fundamental modes (Fig. 3). There are no intersection points between the lines representing the values of effective index for  $E_{11}$  and  $H_{11}$  modes. In order to obtain the degeneracy of the fundamental modes the ratio  $h/H$  of a SOI large rib waveguide must be smaller than 0.5.

In Figures 4 and 5, the dependence of the effective index  $N = \beta/k$  on width  $W$  for a SOI rib waveguide of the  $h/H$  ratio equal to 0.25 is presented. There can be observed two intersection points for the lines representing the values of  $N$  for the fundamental modes  $E_{11}$  and  $H_{11}$ . However, unlike GaAs rib waveguides they are not in the single-mode region [8].

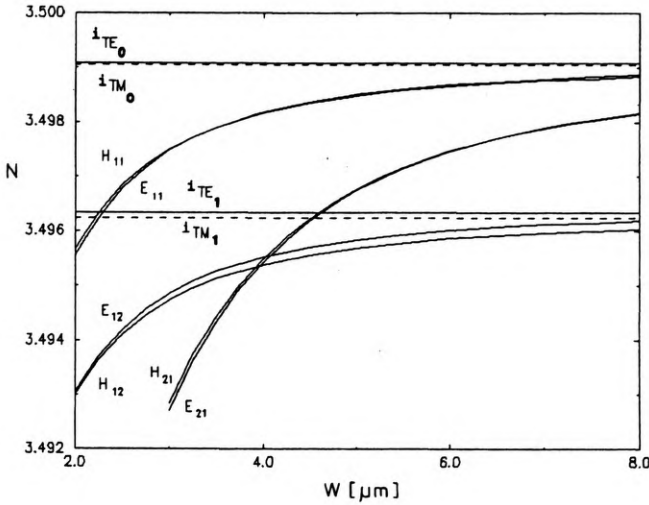


Fig. 4. Dependence of the effective index  $N$  of a SOI rib waveguide on the width  $W$ , where  $h = 2 \mu\text{m}$ ,  $H = 8 \mu\text{m}$  at the wavelength of  $1.3 \mu\text{m}$

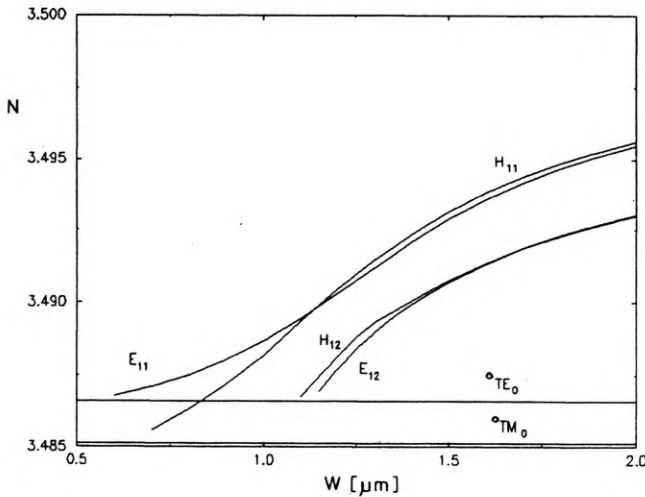


Fig. 5. Dependence of the effective index  $N$  of a SOI rib waveguide on the width  $W$ , where  $h = 2 \mu\text{m}$ ,  $H = 8 \mu\text{m}$  at the wavelength of  $1.3 \mu\text{m}$

In Figure 6, the dependence of birefringence  $\Delta\beta = \beta_x - \beta_y$  on width  $W$  for a typical SOI structure is shown, where  $\beta_x$  and  $\beta_y$  denote the propagation constants of the  $E_{11}$  and  $H_{11}$  modes, respectively. It is seen that when the ratio  $h/H$  is kept constant, the values of birefringence decrease with the width increasing. Maximal value of width  $W$  is, however, restricted by the single-mode condition (1). Consequently, the single-mode condition defines the structure of the smallest birefringence.

It is also observed that the values of the birefringence of a rib waveguide are smaller than the value of the birefringence of the outer slab. Consequently, the

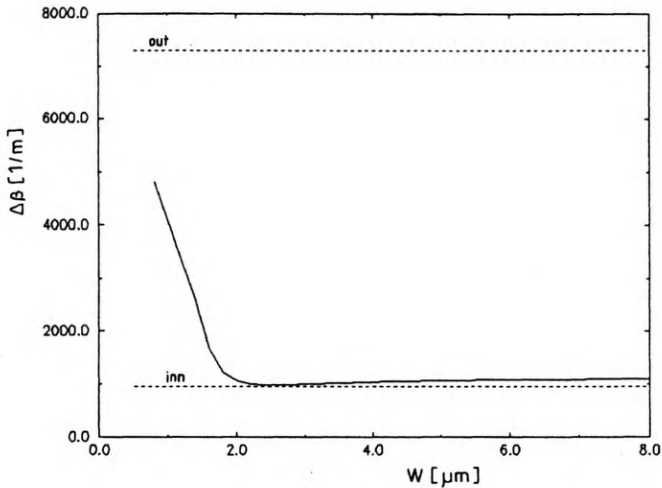


Fig. 6. Dependence of the birefringence  $\Delta\beta$  of a SOI rib waveguide on the width  $W$ , where  $h = 2 \mu\text{m}$ ,  $H = 4 \mu\text{m}$  at the wavelength of  $1.3 \mu\text{m}$

greater the height  $h$ , the smaller the values of birefringence can be achieved. In SOI structures, the values of modal birefringence  $B = \Delta\beta/\beta_x$  of the order of  $10^{-5}$  can be achieved, which is comparable with the values of  $B$  in polarisation independent structures of planar buried rectangular waveguides made of silica [9].

In the Table, the values of birefringence for some typical single-mode structures of silicon SOI (Fig. 2a) and polymer (Fig. 2c) rib waveguides are shown. It is observed that in both cases the values of modal birefringence are of the order of  $10^{-5}$ . It is also seen that the values of birefringence in the case of the silicon core structure are smaller although the refractive index difference is bigger.

Table. The values of birefringence for BCB and SOI rib waveguides at the wavelength of  $1.3 \mu\text{m}$ , the ratio  $h/H = 0.5$ ,  $W/H = 0.4$

$W [\mu\text{m}]$	BCB polymer		SOI	
	$\Delta\beta [1/\text{m}]$	$B \times 10^{-5}$	$\Delta\beta [1/\text{m}]$	$B \times 10^{-5}$
3.2	350	4.71	73	0.432
3.4	295	3.97	61	0.361
3.6	251	3.38	50	0.296
3.8	215	2.89	44	0.260
4.0	186	2.50	37	0.219

In Figures 7, the field distributions of the dominant electric field component of  $E_{11}$  and  $H_{11}$  modes for typical silicon and polymer rib waveguide structures are shown. It is seen that there is only a minor difference between the field distributions for both polarisations. It is also observed that in the case of the silicon rib structure the field is stronger concentrated in the core than for polymer waveguide.

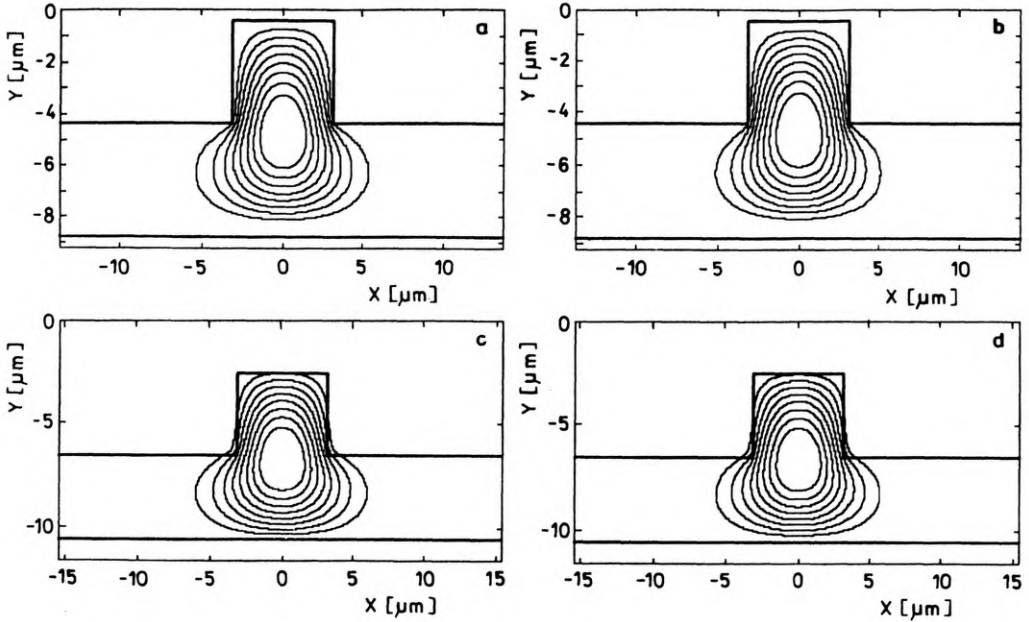


Fig. 7. Field distribution of the dominant electric field component of a fundamental mode,  $h = 4 \mu\text{m}$ ,  $H = 8 \mu\text{m}$ ,  $W = 3.2 \mu\text{m}$  at the wavelength of  $1.3 \mu\text{m}$ : a –  $E_{11}$  mode of a SOI waveguide, b –  $H_{11}$  mode of a SOI waveguide, c –  $E_{11}$  mode of a BCB polymer waveguide, d –  $H_{11}$  mode of a BCB polymer waveguide

### 3. Conclusions

The analysis of the influence of polarisation on the characteristics of rib waveguides has been carried out. It is demonstrated that although the zero value of the modal birefringence cannot be obtained for large single-mode SOI and BCB polymer rib waveguides, it can be reduced to  $10^{-5}$ , which is comparable with the values obtained in polarisation independent silica rectangular waveguides [7].

It has also been shown that the values of birefringence for single-mode silicon rib waveguides are smaller than in the case of the polymer ones, although the refractive index difference in the case of the SOI waveguide is larger.

The distributions of the major field component are almost indistinguishable for both polarisations. It is, however, observed that in the case of the silicon rib waveguide the field is more concentrated in the core than in the case of the polymer based one.

### References

- [1] SOREF R. A., SCHMIDTCHEN J., PETERMANN K., *IEEE J. Quantum Electron.* **27** (1991), 1971.
- [2] SCHUPPERT B., PETERMANN K., *Integrated optics in Si and GeSi-heterostructures*, ECOC-1992, pp. 793–800.

- [3] FISCHER U., ZINKE T., KROPP J. R., ARNDT F., PETERMANN K., *Photonics Tech. Lett.* **8** (1996), 746.
- [4] RITCHIE S., RODGERS P. M., *J. Inst. Electron. Radio Eng.* **57** (1987), 44.
- [5] FISCHBECK G., MOOSBURGER R., TOPPER M., PETERMANN K., *Electron. Lett.* **32** (1996), 212.
- [6] MAJEWSKI A., SUJECKI S., *The analysis of the rib-lightguide structures by finite difference method*, Intern. Seminar on Environment Modelling, Riga'95, Latvia, pp. 257–266.
- [7] SUJECKI S., BENSON T. M., SEWELL P., KENDALL P. C., *IEEE J. Lightwave Technol.* **16** (1998), 1329.
- [8] CHIANG K. S., WONG W. P., *Electron. Lett.* **32** (1996), 1098.
- [9] SUZUKI S., INOUE Y., OHMORI Y., *Electron. Lett.* **30** (1994), 643.

*Received October 5, 1998*